Top Catal (2007) 46:363–373
DOI 10.1007/s11244-007-9013-8

ORIGINAL PAPER

The Importance of Strongly Bound Pt–CeO_x Species for the Water-gas Shift Reaction: Catalyst Activity and Stability Evaluation

Danny Pierre · Weiling Deng · Maria Flytzani-Stephanopoulos

Published online: 27 November 2007
© Springer Science+Business Media, LLC 2007

Abstract We demonstrate ways to prepare active and stable Pt–CeO_x catalysts for the water-gas shift reaction (WGSR). Various synthesis protocols are shown to work; the best being the coprecipitation/gelation method, which suppresses the crystal growth of ceria during calcination by the incorporation of some platinum in the bulk oxide. Metallic platinum nanoparticles are not necessary for an active WGSR catalyst. Reaction light-off occurs at ~120 °C, where Pt^{2+} species bound to ceria are still present. No activation period, and no hysteresis phenomena were found. During reaction at reducing conditions, some Pt is reduced, but it is reoxidizable. The stability of these low-content (<2 at.%) Pt/CeO_x catalysts is high even in realistic reformate gas streams. To avoid cerium(III) hydroxycarbonate formation at room temperature-shutdown with water condensation, a small amount (~1%) of gaseous oxygen is added to the reaction gas mixture. Cyclic shutdown/startup operation is thus possible without catalyst degradation.

Keywords Cerium oxide · Platinum · Water-gas shift · TPR · XPS · Fuel cells · Catalyst deactivation · Carbonate

1 Introduction

Cerium oxide carrying small amounts of Au, Pt, Cu or other metals shows excellent catalytic activity for a variety of redox reactions. As a carrier of Pt-group metals, it is an indispensable component of the three-way catalyst in automotive engine exhausts. Properly stabilized with dopants, such as rare earth or zirconium oxides, ceria has a large oxygen storage capacity [1] and is a suitable carrier of platinum and nickel catalysts for the high-temperature partial oxidation and steam reforming reactions of natural gas and liquid fuels to produce synthesis gas without carbon deposition [2]. While the high metal dispersion that can be achieved on ceria is not unique to this oxide support, what appears to be unique is the ability of ceria to stabilize oxidized metal species on its surface and subsurface layers [3–8]. In this article, we review the catalytic properties and stability of these species for the water-gas shift reaction (WGSR) at low temperatures. This is an important reaction in fuel processing that enriches the hydrogen content of reformate gas streams and removes carbon monoxide, the latter being a strong poison of the current generation of PEM fuel cell anode catalysts.

It is well established in the literature that addition of Pt metals on ceria dramatically enhances the reducibility of the surface oxygen of ceria. This was shown more than 20 years ago by Yao and Yu Yao [9]. Pt-group metals supported on a high surface area ceria are much more active for the CO oxidation [10] and the WGSR [7, 11] than if loaded on annealed microcrystalline ceria or on alumina, as was shown by the Gorte's group. The same is true for CuO/CeO_2 [3, 4, 12–14]. In recent years, our group has focused on evaluating nanoscale Au/ceria catalysts for low-temperature oxidation reactions. After establishing the high activity of Au/ceria for the CO and methane oxidation [3, 4], we were first to show that Au/ceria has very high activity for WGSR [15]. This was subsequently verified by several other literature reports, e.g., [16, 17]. A cooperative effect of ceria was invoked to explain why the ceria properties (surface area, crystal size) seemed to matter [15]. More recently, we were able to document the

D. Pierre · W. Deng · M. Flytzani-Stephanopoulos (✉)
Department of Chemical and Biological Engineering,
Tufts University, 4 Colby St., Medford, MA 02155, USA
e-mail: maria.flytzani-stephanopoulos@tufts.edu

importance of the interaction between gold and the oxygen of ceria [7, 8, 18] by showing that only the gold species embedded or otherwise associated with ceria [Au_n–O–Ce] are the active sites for WGSR [7]. The number of these bound gold species that can be carried by ceria is increased as the crystal size of ceria is decreased [8]. Similarly, oxidized clusters of Pt bound to ceria, [Pt_n–O–Ce], were found after removing the platinum nanoparticles from the ceria surface by cyanide leaching; and all the platinum had diffused in the subsurface layers of ceria [7, 19]. In earlier work, we had noticed similar effects with the Cu/ceria oxidation catalysts; namely, that only a small amount of copper (<2 at.%) strongly bound to ceria (non-leachable) was responsible for the CO oxidation reaction [3, 4].

A novel synthesis approach aimed at demonstrating and maximizing the interaction between Pt and ceria was reported by Tsang's group in 2005 [20]. Encapsulation of platinum particles inside a nanoscale shell of ceria was achieved by a reverse microemulsion technique. The resulting material showed excellent activity for the WGS reaction, while the undesired methanation reaction was suppressed by not exposing the metallic Pt sites.

Nanoscale ceria has a much higher concentration of surface oxygen defects than microcrystalline ceria and much higher conductivity. This is true both for the bulk material [21] as well as for thin films of ceria [22]. The surface Ce–O bond is weakened by the presence of a metal and this oxygen becomes reactive at low temperatures. Addition of gold, platinum, etc. increases the available oxygen on the surface, if preparation conditions are properly controlled. Recently, the Corma group has also reported on the importance of nanoscale ceria and characterized the types of excess active oxygen on the surface of gold/nanoceria materials [23, 24].

Deactivation with time-on-stream and/or shutdown/restartup operation has been reported for WGS catalysts based on ceria [8, 25–29] or copper oxide [30]. The noble metal/ceria materials are superior to commercial low-temperature shift catalysts based on Cu/ZnO in that they are non-pyrophoric, do not require activation, do not catalyze the methanation reaction; and are thus a better candidate for application to small-scale fuel cells, undergoing frequent air purges. However, deactivation of the Pt metal/ceria catalysts with time-on-stream in realistic reformate-gas streams has been reported and attributed to various reasons, such as metal-induced over-reduction of ceria [26], precious metal sintering after high-temperature reaction aging of Pd and Pt/CeO_2 catalysts [27] and carbonate formation [28]. Finally, a different type of deactivation was found in cyclic operation, mimicking the frequent shutdowns to room temperature followed by re-start of a realistic fuel cell system. Severe deactivation due to carbonate formation has been reported both for Pt/CeO_2 [29] and Au-ceria [8, 19] after shutdown in the full gas mixture with water condensation. The problem lies with ceria, which forms Ce (III) hydroxycarbonate under these conditions [8]. Doping ceria with zirconia was found to improve the stability of undoped ceria [29]. While activity can be recovered by reoxidation of the catalyst in air at high temperatures (>450 °C) [8, 29], this scheme is not practical in a continuous operation of a fuel cell system.

A practical, in situ remedy of the deactivation problem of ceria upon WGS shutdown was proposed earlier this year by Deng et al. [31]. This was based on the information that Au/CeO_x is an excellent catalyst for the preferential CO oxidation reaction (PROX) [32] and is *not* deactivated in cyclic shutdown/startup PROX operation when exposed to practically the same gas mixture as for WGS, except for the presence of gaseous oxygen. Addition of a small amount of oxygen in the WGS reaction gas mixture was then tried and shown to prevent the Ce (III) hydroxycarbonate formation. Full stabilization of the Au/ceria catalyst was demonstrated both in continuous operations at temperatures up to 300 °C, and in cyclic room temperature shutdown/reheat to 150 or 300°C [31, 33].

With this background, it is plausible to approach the design of novel ceria-based catalysts for WGS reactors coupled to fuel cell systems with a two-prong objective: (i) to investigate ways to increase the amount of fully bound Pt- or Au- on ceria, which would in turn increase the rate of the WGSR; and (ii) to examine the catalyst activity and stability in realistic reaction gas streams and in cyclic operation, including shutdown to ambient conditions. In the present paper we show this for Pt–CeO_x catalysts.

2 Experimental

2.1 Catalyst Preparation

Lanthanum-doped ceria and undoped ceria materials were prepared by the urea gelation/co-precipitation (UGC) method. Details about this preparation technique can be found elsewhere [7, 13]. Low-content platinum–ceria samples were prepared by one-pot synthesis using UGC, and by incipient wetness impregnation (IMP), and deposition–precipitation (DP) on ceria particles prepared by the UGC method and calcined at 400 °C. All reagents used in catalyst preparation were analytical grade. The samples reported here are denoted as a%PtCeO_x or a%PtCeLaO_x where a is the atomic percent of platinum in the sample: $100 \times (Pt/MW_{Pt})/(Pt/MW_{Pt} + Ce/MW_{Ce} + La/MW_{La})$, CeLa$O_x$ is ceria doped with10 at.% La.

For IMP samples, the ceria support was impregnated with a solution of chloroplatinic acid at room temperature (RT). A measured amount of solution carrying the required metal ion concentration was added dropwise to fill the pore

volume of the solid support. This was followed by drying the material in a vacuum oven at 60 °C for 10 h to remove water and allow good coating of the metal precursor on the pore surface. The dried material was calcined at 400 °C with a heating rate of 2 °C/min starting from RT and stayed at 400 °C for 10 h.

In the DP method, two different platinum precursors were used: tetra-amine platinum(II) nitrate, $(NH_3)_4Pt(NO_3)_2$, and hydrogen hexacholoroplatinate(IV) hydrate, H_2PtCl_6. In both cases, the solution containing the desired amount of platinum was added dropwise into an aqueous slurry of a previously UGC-prepared ceria. Prior to this addition, the pH of the slurry was adjusted to 2 before adding H_2PtCl_6 using 1M HNO_3 and to 12 before adding $(NH_3)_4Pt(NO_3)_2$ using 1 M NaOH, respectively. After aging for 1 h, the precipitate was filtered and washed with deionized water. The resultant material was then dried and calcined as described above.

Some materials were leached with 2%NaCN–NaOH solution (pH > 12) at ~90 °C reflux in an oil bath for 24 h [7] to remove weakly bound platinum species from the ceria surface. Leached samples were washed with deionized water three times; dried in a vacuum oven for 10 h and heated in air at 400 °C for 2 h.

2.2 Characterization Techniques

The BET surface area was measured by single-point N_2 adsorption/desorption cycles in a Micromeritics Pulse ChemiSorb 2705 flow apparatus. Bulk composition analysis of the catalysts was conducted in an Inductively Coupled Plasma Optical Emission Spectrometer (ICP-OES, Leeman Labs Inc.). XPS and XRD analyses were performed at the MIT Center for Materials Science and Engineering. For XPS, a Kratos AXIS Ultra Imaging X-ray Photoelectron Spectrometer with a resolution of 0.1 eV was used to determine the atomic metal ratios of the surface region and the oxidation state of platinum in selected catalysts. Samples in powder form were pressed on a double-side adhesive copper tape for analysis. All measurements were carried out at room temperature without any sample pre-treatment. An Al Kα X-ray source was used in this work. All binding energies were adjusted to the C1s peaks at 285 eV. An adjacent neutralizer was used to minimize the static charge on the samples. XRD analysis was performed on a Rigaku 300 instrument with a rotating anode generator and a monochromatic detector. Cu Kα1 radiation was used with a power setting of 60 kV and 300 mA. Typically, a scan rate of 2°/min with 0.02° data interval was used. Tungsten was used as an internal standard. The software TOPAS (Bruker) was used to perform microstructure analysis.

2.3 Testing Apparatus and Procedures

Temperature-programmed reduction by hydrogen (H_2-TPR) was conducted in a Micromeritics Pulse ChemiSorb 2705 instrument equipped with a thermal conductivity detector to detect H_2 consumption. The as prepared materials (0.5 g sample) in fine powder form were purged in He for 0.5 h before starting the TPR at a rate of 5 °C/min from RT to 400 °C in a 20% H_2/N_2 gas mixture (50 cm^3/min (NTP)). In cyclic H_2-TPR experiments, a He sweep immediately followed the first TPR test, the sample was reoxidized in the 20% O_2/He gas mixture (50 cm^3/min (NTP)) at 350 °C for 30 min; cooled to RT in the oxygen gas mixture; then purged in He before starting the second TPR cycle.

WGSR tests were conducted at atmospheric pressure with the catalyst in powder form (<150 μm). A quartz tube (o.d. = 1 or 0.5 cm) with a porous quartz frit supporting the catalyst was used as a packed-bed flow reactor. Water was injected into the flowing gas stream by a calibrated syringe pump and vaporized in the heated gas feed line before entering the reactor. A condenser filled with ice was installed at the reactor exit to collect water. The feed and product gas streams were analyzed by a HP-6890 gas chromatograph (GC) equipped with a thermal conductivity detector (TCD). A Carbosphere (Alltech) packed column (6 ft × 1/8 in.) was used to separate O_2, CO, H_2, and CO_2. No methane was produced under any of the operating conditions used in this work.

3 Results and Discussion

3.1 Characterization

Table 1 lists the physical properties of the as prepared materials. Catalysts made by DP or IMP have similar mean particle size of ceria as the support itself, around 7 nm for CeO_2 or 5 nm for $CeLaO_x$. However, UGC-prepared platinum–ceria samples have a much smaller mean particle size of ceria (Table 1). For example, in the 1.1 at.% and 5.3 at.% $PtCeO_x$, the ceria <111> particle size is 5.1 nm and 3.7 nm, respectively, which is much smaller than the 7.1 nm particle size of platinum-free ceria prepared by UGC. This is a clear indication that the presence of Pt can inhibit cerium oxide particle growth during the calcination step. However, it is difficult to identify if there is platinum ion substitution in the ceria lattice because the radius of Pt^{2+} (octahedral coordinated) is 0.94 Å [34], very close to that of Ce^{4+} (0.97 Å). An appreciable expansion of the ceria lattice constant is seen in Table 1 for these samples. This is attributed to the presence of Ce^{3+}, which is a larger ion than Ce^{4+}, its

Table 1 Physical properties of platinum–ceria materials[a]

Sample	BET	Bulk composition[b] (at. %)			Surface composition[c] (at. %)			Crystallite size[d] (nm)			Lattice constant[e] (Å)	
	S.A.(m^2/g)	Pt	Ce	La	Pt	Ce	La	Pt	CeO_2		CeO_2	
									<111>	<220>	<111>	<220>
2.2%PtCeLaO$_x$(IMP)	151.1	2.20	89.32	8.48	NM	NM	NM	ND	5.2	5.0	5.422	5.422
0.7%PtCeLaO$_x$(IMP,NaCN)	162.9	0.74	90.71	8.55	NM	NM	NM	ND	5.3	5.0	5.432	5.432
1.2%PtCeO$_x$(IMP)	156.0	1.22	98.78	0	0.59	99.41	0	ND	6.3	7.6	5.417	5.415
0.8%PtCeO$_x$(DP,pH2)	144.0	0.82	99.20	0	0.51	99.49	0	ND	6.4	7.8	5.413	5.421
0.8%PtCeO$_x$(DP,pH2)[f]	119.0	0.82	99.20	0	0.62	99.38	0	ND	6.6	7.9	5.435	5.418
0.3%PtCeO$_x$(DP,pH12)	140.0	0.30	99.70	0	0.12	99.88	0	ND	6.6	7.5	5.418	5.416
5.3%PtCeO$_x$(UGC)	140.7	5.32	94.68	0	3.5	96.5	0	ND	3.7	3.2	5.413	5.436
5.3%PtCeO$_x$(UGC)[f]	NM	5.32	94.68	0	3.5	96.5	0	ND	3.8	3.5	5.431	5.473
1.1%PtCeO$_x$(UGC)	167.9	1.07	98.93	0	0.95	99.05	0	ND	5.1	4.6	5.442	5.401
CeLaO$_x$(UGC)	156.9	0	92.62	7.38	0	ND	ND	–	5.1	4.8	5.438	5.442
CeO_2 (UGC)	140.5	0	100	0	0	100	0	–	7.1	6.6	5.415	5.416

[a] All samples calcined at 400 °C in air for 10 h, except the leached samples for 2 h

CeLaO$_x$: 10 at.%La-doped ceria, calcined at 400 °C, 10 h; ND: non-detectable; NM: not measured

[b] Bulk composition was determined by Inductively Coupled Plasma (ICP) emission spectrometry

[c] Surface composition was determined by XPS

[d] The crystallite size was determined from XRD data with the Scherrer equation

[e] The lattice constant was determined by the expression $\alpha = \sqrt{h^2 + k^2 + l^2}(\lambda/2 \sin \theta)$

[f] Sample was used for 17 h at 300 °C in the reaction gas mixture of 11%CO–26%H_2O–26%H_2–7%CO_2–He

fraction increasing as the size of nanoscale ceria is decreased [35].

The low-content platinum/ceria samples prepared by the DP, IMP, and UGC methods contain oxidized Pt species as identified by XPS in Fig. 1. 0.8%PtCeO$_2$ (DP), 0.3%PtCeO$_2$ (DP), and 1.2%PtCeO$_2$ (IMP) have mainly Pt^{2+} species (binding energy at 72.6 and 76.0 eV) while both UGC samples have a mix of Pt^{2+} and Pt^{4+} (binding energy at 74.0 and 77.4 eV). All of them have negligible Pt^0 (binding energy at 70.9 and 74.3 eV). The higher content 5.3%PtCeO$_2$ (UGC) sample still shows all of its platinum in 2^+ and 4^+ oxidation states. This is the sample with the smallest average particle size of ceria (Table 1). The surface platinum content of the samples was also determined by XPS and can be seen in Table 1. The fraction of Pt on the surface is less than the bulk value. A lot of platinum is subsurface in ceria, even in the sample prepared with 5.3% Pt by the UGC technique. No platinum phases were detected by XRD in any of the PtCeO$_x$ samples shown in Table 1, including the high content 5.3%PtCeO$_2$, indicating the platinum is present in highly dispersed small clusters in cerium oxide. Taken together the XPS data of Fig. 1 and the sample analysis of Table 1, provide evidence that the as prepared materials comprise oxidized platinum clusters strongly bound to nanoscale ceria.

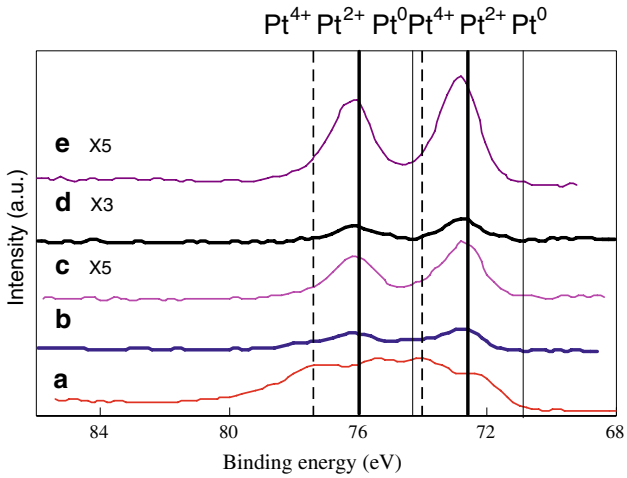

Fig. 1 XPS of Pt_{4f}–Pt–CeO$_x$ samples, as prepared, after air calcination at 400 °C. (a) 5.3%PtCeO$_x$ (UGC); (b) 1.1%PtCeO$_x$ (UGC); (c) 0.8%PtCeO$_x$ (DP, pH2); (d) 0.3%PtCeO$_x$ (DP, pH12); (e) 1.2%PtCeO$_x$ (IMP). X5 and X3 is signal magnification

3.2 WGS Reaction Activity and Stability

Figure 2 shows steady-state CO conversions in the WGS reaction over the platinum–ceria catalysts prepared by different methods in a product-free feed gas mixture containing 2%CO and 10.7%H_2O in helium. For each run,

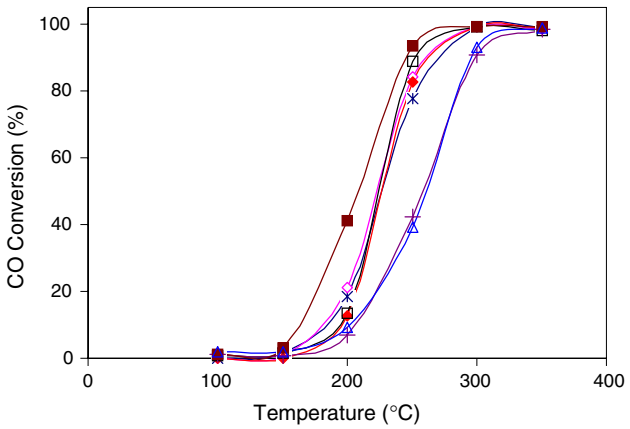

Fig. 2 WGS reaction light-off over platinum–ceria catalysts; steady-state conversion measurements. Gas mixture: 2%CO–10.7%H_2O–He; contact time: 0.09 g s/cc. Open Triangles—2.2%PtCeLaO$_x$ (IMP); Open squares—0.7%PtCeLaO$_x$ (IMP, NaCN); Asterisks—0.8%PtCeO$_x$ (DP, pH2); Open diamonds—1.2%PtCeO$_x$ (IMP); Crosshairs—0.3%PtCeO$_x$ (DP, pH12); Closed Squares—5.3%PtCeO$_x$ (UGC); Closed diamonds—1.1%PtCeO$_x$ (UGC)

0.1 g sample was tested in ascending temperature mode (50 °C-increments) followed by descending temperature to check for potential hysteresis phenomena and deactivation. Each steady-state test was run for 1.5 h. The reaction light-off temperature was similar for all the samples, but the high-temperature conversion varied for different samples, likely due to different structural evolution of their surfaces. The high surface Pt-content 5.3%Pt–CeO$_x$ catalyst made by UGC showed the highest CO conversion at all temperatures at the conditions of Fig. 2. At 300 °C, the CO conversion was at least 90% over all catalysts.

We further evaluated the catalysts in a realistic reformate gas composition. It is of interest both from a practical as well as a fundamental point of view to check the activity and stability of these PtCeO$_x$ samples in a gas with a large content of hydrogen and also in the presence of CO_2. Table 2 shows the steady-state reaction rates measured at 250 °C over these catalysts at CO conversions less than 20% to avoid mass transfer effects. The IMP samples are similarly active. The UGC samples have good rates, the 5.3%PtCeO$_x$ sample showing the highest rate, which we attribute to the higher amount of Pt present in active form in this sample. If we normalize the rates by the surface amount of Pt measured by XPS on the as prepared samples, as a first-order approximation, we can calculate the turnover frequencies (TOF) of the reaction. Since by XRD no diffraction pattern was found for Pt in any of the samples and the XPS analysis found all the platinum in oxidized form, the TOF calculation assumed that the surface Pt determined by XPS was fully dispersed (see foot notes in Table 2). As shown in the last column of Table 2, a value of TOF $= 0.15 \pm 0.06$ s^{-1} is found for all samples at 250 °C. Of course, this is only an approximate value, as the surface amount and the dispersion of platinum may vary with time-on-stream for some or all of these samples. But it is interesting that all samples have similar TOFs and also similar apparent activation energies, $E_a = 81.0 \pm 6.8$ kJ/mol. If we compare the ceria properties of the catalysts

Table 2 WGS reaction activity measured in a reformate gas mixture[a]

	Apparent activation energy (kJ/mol)	Reaction rate[c] (μmol $CO_2/g_{cat}/s$)	TOF[e] (s^{-1})
2.2%Pt CeLaO$_x$ (IMP)	80.7	7.2	N/A
0.7%Pt CeLaO$_x$ (IMP,NaCN)	84.9	6.5	N/A
1.2%PtCeO$_x$ (IMP)	83.2	5.7	0.17
0.8%PtCeO$_x$ (DP,pH2)	85.8	4.0	0.13
0.3%PtCeO$_x$ (DP,pH12)	72.7	1.5	0.21
5.3%PtCeO$_x$ (UGC)	85.4	20.7	0.10
1.1%PtCeO$_x$ (UGC)	84.6	6.2	0.11
3.7%PtCeLaO$_x$ (IMP)[b]	74.2	10.0	0.11
2.7%PtCeLaO$_x$ (IMP,NaCN)[b]	75.2	16.1	0.16
1.5%PtCeLaO$_x$ (IMP,NaCN)[b]	75.0	6.3	0.21
CeLaO$_x$ (UGC)	82.7	0.02[d]	–

[a] 11%CO–8%CO_2–26%H_2–26%H_2O–bal.He

[b] Data adapted from Ref. [7]

[c] 250 °C, 1 atm

[d] Rate extrapolated from high temperature rate measurements

[e] Turnover frequency; based on the initial amount of surface Pt species found by XPS, see Table 1 $\mathrm{TOF}(s^{-1}) = r\left(\frac{\mathrm{mol}}{g_{cat}*\mathrm{sec}}\right) * \left(\frac{g_{cat}}{\mathrm{mass\ of\ Pt_{on\ cat\ surface}}}\right) * \left(\frac{M_w\ \mathrm{of\ Pt}}{\mathrm{Fraction\ of\ surface\ atoms}}\right)$

listed in Table 1, the particle size of CeO_2 is a key variable. The samples prepared by the UGC method have the smallest cerium oxide particle size and can retain more oxidized platinum species on their surface and sub-surface layers which correlates well with their higher reaction activity. Similar results were reported for gold/ceria catalysts [7, 8, 15]. A much higher WGSR activity of Pt-metals deposited on nanoscale ceria films was first reported by the Gorte group [11].

The activity and stability of some of the above catalysts was further evaluated in the same WGSR gas mixture of 11%CO–26%H_2O–26%H_2–7%CO_2–He at 300 °C for 17 h. As can be seen in Fig. 3a, the stability of $PtCeO_x$ is generally very good. Unlike what has been reported in the literature for some other Pt/CeO_2 catalysts [26], no drastic initial deactivation is observed for any of the samples shown in Fig. 3a. However, there are some activity differences among our samples that can be traced to their different preparation and structure. The 0.7%$PtCeLaO_x$ (IMP, NaCN) and 0.8%$PtCeO_x$ (DP) catalysts appear less active and stable than the1.1%$PtCeO_x$ (UGC) and the 1.2%$PtCeO_x$ (IMP) sample. The CO conversion falls from ~60% to ~50% over 17 h for the former two catalysts, while it remains constant at ~80% for the latter. The best performance is shown by the 5.3%$PtCeO_x$ (UGC) sample, which reaches the equilibrium CO conversion of 92%, and shows excellent stability with time-on-stream at 300 °C.

XP Pt_{4f} spectra of the fresh and used 0.8%$PtCeO_x$ (DP) catalyst are shown in Fig. 3b. Some metallic Pt is now found in the used sample. Peak deconvolution shows that over 50% of the Pt is still in oxidized form. The BET surface area of the used sample is 119 m^2/g, lower than the initial value of 144 m^2/g. (Table 1). This may explain the ~20% loss in activity. The lattice constant is higher in the used catalyst indicating that a higher amount of Ce^3, is likely present in the used than the fresh sample causing lattice expansion as discussed above.

Figure 3c presents the XP Pt_{4f} spectra for the as prepared and used 5.3%$PtCeO_x$ (UGC) catalyst. The used sample lost most of its Pt^{4+} species. Pt^{2+} species now dominate, while no metallic platinum has formed. This sample is the most active and stable under the conditions of Figs. 2 and 3. The absence of Pt^{4+} has no effect on the catalyst stability. Thus, Pt^{2+} species are responsible for the observed catalyst activity. Comparing these data with the 0.8%$PtCeO_x$(DP) catalyst, we can surmise that the deactivation of the latter with time-on-stream (Fig. 3a) is due to accumulation of Pt^0 (Fig. 3b). Metallic platinum may in turn cause the annealing of ceria oxygen vacancies and the loss of ceria surface area.

From the above evaluation, the catalyst that consistently showed the best activity and stability is the UGC-prepared 5.3%$PtCeO_x$. This has the smallest particle size of ceria

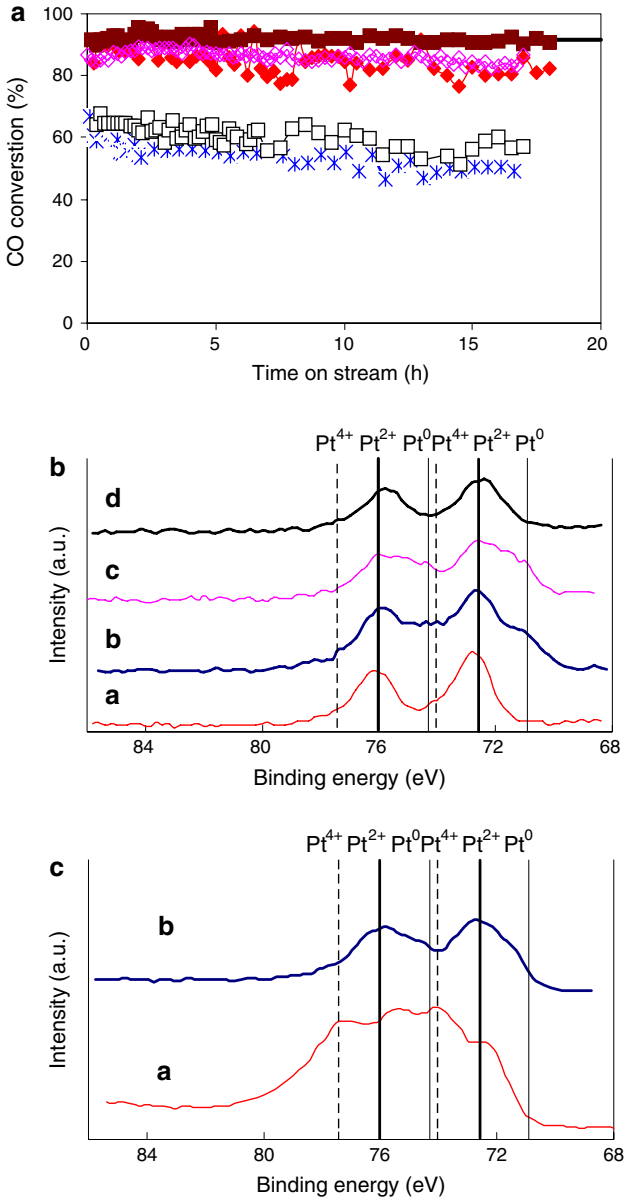

Fig. 3 (**a**) WGS stability of $PtCeO_x$ catalysts at 300 °C. Gas mixture: 11%CO–26%H_2O–26%H_2–7%CO_2–He; sample load 0.5 g; S.V. = 50,000/h (NTP). Solid line—Equilibrium conversion; Open squares—0.7%$PtCeLaO_x$ (IMP, NaCN); Open diamonds—1.2% $PtCeO_x$ (IMP); Asterisks—0.8%$PtCeO_x$ (DP, pH2); Closed squares—5.3%$PtCeO_x$ (UGC); Closed diamonds—1.1%$PtCeO_x$ (UGC). (**b**) XPS of Pt_{4f}—0.8%$PtCeO_x$ (DP,pH2). (a) as-prepared; (b) used at the conditions of **a**, after 17 h at 300°C; (c) after H_2-TPR; (d) reoxidized after H_2-TPR by oxygen at 350°C for 0.5 h. (**c**) XPS of Pt_{4f}—5.3%$PtCeO_x$ (UGC). (a) as-prepared (b) used at the conditions of **a**, after 17 h at 300°C

(Table 1) and can stabilize more platinum in the desired strongly bound Pt_n–O–Ce form. Similar to what we have previously reported for Au on nanoscale CeO_2 [7, 8, 15], the UGC preparation method increases the concentration of these species and higher reaction rates are possible. The

TOF of the WGS reaction measured at 250°C is the same for all samples (Table 2).

3.3 Reducibility in H_2

It is of interest to evaluate the reducibility of the Pt–CeO_x catalysts and investigate the potential correlation of their reducibility with their WGSR activity. The literature on the subject is rather confusing. The effect of weakening the surface O–Ce bond by addition of a Pt-group metal on ceria is well accepted and has been documented in numerous reports ever since it was first demonstrated by Yao and Yu Yao [9]. However, over-reduction of ceria may not always be advantageous. While the presence of metallic platinum and gold nanoparticles on ceria causes a dramatic reducibility enhancement of the surface oxygen of ceria to temperatures below 100 °C, oxidized species of Pt and Au strongly bound to ceria are less reducible [7, 8, 15, 19, 20]. Yet, that does not mean that the latter are less active. On the contrary, these rather than the metallic Au or Pt nanoparticles are the active species for some redox reactions, such as the WGSR [7]. For other reactions, such as the CO oxidation reaction by dioxygen, the opposite may hold true [36].

None of the samples prepared here contains metallic platinum as verified also by H_2-TPR, in Figs. 4 and 5, which show absence of the characteristic low-temperature reduction peak. Instead, oxygen reduction begins at temperatures approaching or higher than 200 °C. An exception is seen in Fig. 5a for 5.3%PtCeO_x, which begins to reduce at ~120 °C and two different types of surface oxygen are distinguishable. Reduction peak temperatures are listed in Table 3 for the first and second cycles of H_2-TPR. The second TPR cycle is typical for metallic Pt on ceria, as can be seen by the very sharp, low-temperature (<100 °C) reduction peaks. A third cycle (not shown) was similar to the second. Thus, after the first treatment in H_2 up to 400 °C, metallic Pt nanoparticles are formed. Unlike gold-ceria materials [8], the reduced platinum–ceria samples can not be reoxidized at ambient temperature by oxygen or water vapor.

The presence of metallic platinum after the first TPR cycle was checked by XPS on the 0.8%PtCeO_x (DP) sample. As can be seen in Fig. 3b, line c, after the test in H_2-TPR up to 400 °C, the Pt_{4f} binding energies shifted to lower values, indicative of metallic Pt formation. A 350 °C-oxidation in 20%O_2 can drive most of the Pt^0 back to Pt^{2+} (Fig. 3b, line d). However, the structure is not fully reversible. In Table 3, the second cycle of TPR of

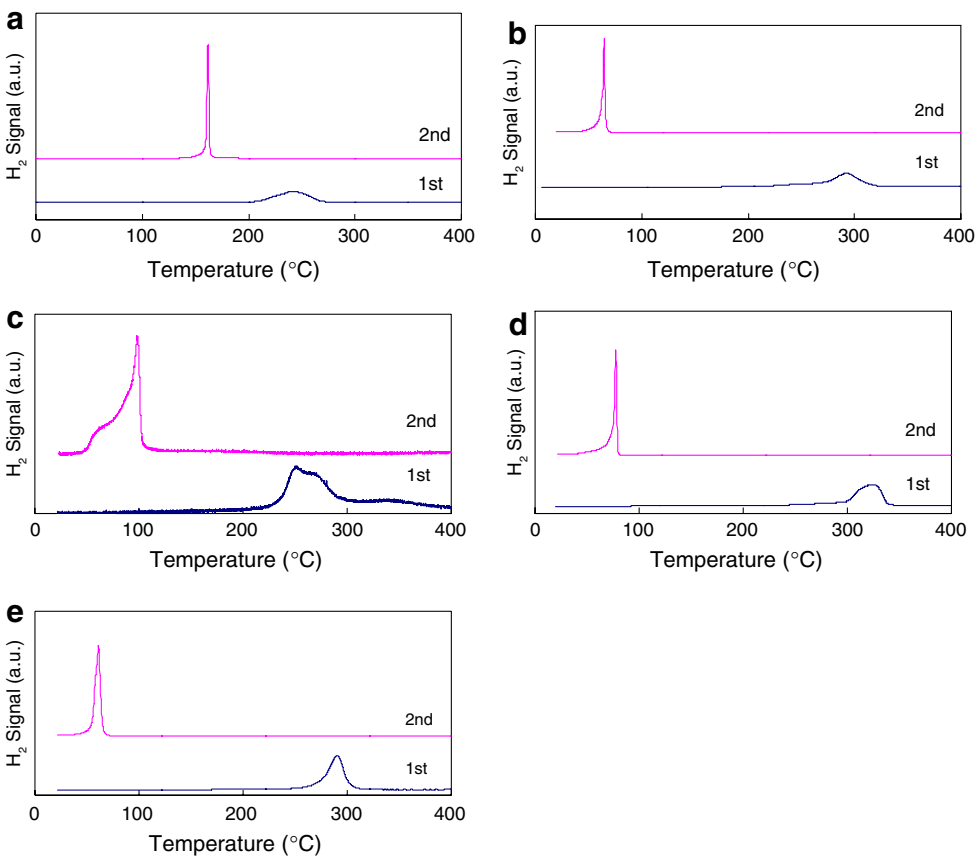

Fig. 4 H_2-TPR cycles of (**a**) 2.2%PtCeLaO_x (IMP); (**b**) 0.7%PtCeLaO_x (IMP, NaCN); (**c**) 1.2%PtCeO_x (IMP); (**d**) 0.8%PtCeO_x (DP pH2); (**e**) 0.3%PtCeO_x (DP pH12). Samples were purged in He at RT for 0.5 h before the first cycle. Test: 20%H_2/N_2; 50 cm^3/min (NTP); 5°C/min. The subsequent cycle was run after 20%O_2/He reoxidation at 350 °C for 0.5 h and purge with He

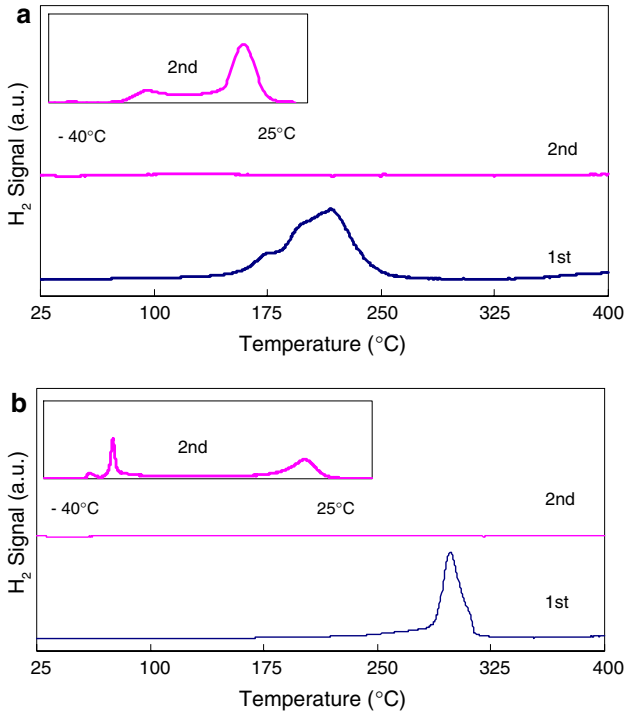

Fig. 5 H_2-TPR cycles of (**a**) 5.3%$PtCeO_x$ (UGC); (**b**) 1.1%$PtCeO_x$ (UGC). Samples were purged in He at RT for 0.5 h before the first cycle. Test: 20%H_2/N_2; 50 cm^3/min (NTP); 5 °C/min. The subsequent cycle was run after 20%O_2/He reoxidation at 350 °C for 0.5 h and purge with He

0.8%$PtCeO_x$ shows hydrogen consumption of only 638 μmol/g_{cat}, a 40% loss compared to the first cycle. In contrast, exposure of the catalyst to the full reformate gas mixture (11%CO–26%H_2O–26%H_2–7%CO_2–He) at 300 °C for 17 h retains more oxidized platinum in the sample than exposure to hydrogen (Line b in Fig. 3b). This is corroborated by the TPR data for the used catalyst after 17 h time-on-stream (not shown). The hydrogen consumption over the reaction-used material is 954 μmol/g_{cat}, a little less than the fresh, but much higher than in the second TPR cycle (638 μmol/g_{cat}, Table 3).

The 5.3%$PtCeO_x$ (UGC) sample shows the highest H_2 consumption value of 2040 μmol/g_{cat}, while the 1.1%$PtCeO_x$ (UGC) sample follows with 1060 μmol/g_{cat}. Following reoxidation of these samples at 350 °C, a second cycle of TPR found their reduction profiles had shifted dramatically to temperatures lower than ambient. To capture this reduction, a dry ice-ethanol bath was used to lower the temperature to −40 °C and thereby suppress the immediate room temperature reduction. The cyclic reduction profiles of the 5.3%$PtCeO_x$ (UGC) sample are shown in Fig. 5a. There are two major reduction peaks seen as the sample heats in the H_2 test gas up to room temperature from the sub-zero temperature giving a total reduction of 1,339 μmol/g_{cat}. No further reduction is observed from 25 °C to the final temperature of 400 °C.

An in situ H_2 reduction up to 400 °C was performed on both the UGC and the 2.2%$PtCeLaO_x$ (IMP) samples prior to exposure to WGS product-free reaction gases (see Fig. 6a). Following this in situ reduction process, all samples were more active for WGSR than the fresh materials. This increased activity of the samples may be caused by either: (1) activation of the catalyst by the H_2 gas; or (2) exposure of the active sites by the removal of carbonates from the surface. To answer this, a fresh batch of 5.3%$PtCeO_x$ was oxidized in situ at 350 °C for 30 min prior to exposure to the WGSR product-free gas. As can be seen in Fig. 6b, the preoxidized sample has a similar activated performance to that of the in situ reduced material. This demonstrates the surface carbonate decomposition as the reason for the catalyst activation shown in Fig. 6a and b.

The in situ reduced and WGSR used 5.3%$PtCeO_x$ and 1.1%$PtCeO_x$ UGC samples were further subjected to a TPR experiment. A helium purge at RT for 0.5 h was the only pretreatment of the used 5.3%Pt–CeO_x sample before starting the TPR test. Unlike its behavior in cyclic TPR (Fig. 5a), the reaction used 5.3%Pt material had two distinct regions of reduction: a sub-RT and a high temperature one (Fig. 6c). Integration of the sub-RT reduction peak gave a consumption of H_2 of 581 μmol/g_{cat} and the high temperature one 1193 μmol H_2/g_{cat}. On the other hand, the used 1.1%$PtCeO_x$

Table 3 Reducibility of Pt–CeO_x materials[a]

Catalyst	H_2-TPR			
	Cycle 1		Cycle 2	
	T_r^b (°C)	H_2 consumption (μmol/g)	T_r^b (°C)	H_2 consumption (μmol/g)
2.2%$PtCeLaO_x$(IMP)	241	1099	162	1121
0.7%$PtCeLaO_x$ (IMP, NaCN)	294	809	65	505
1.2%$PtCeO_x$(IMP)	261	988	81	744
0.8%$PtCeO_x$(DP,pH2)	325	1037	78	638
0.3%$PtCeO_x$(DP,pH12)	293	800	62	572
5.3%$PtCeO_x$(UGC)	217	2040	<25	1339
1.1%$PtCeO_x$(UGC)	298	1060	<25	947

[a] Samples were purged in He at RT for 0.5 h before the first cycle. The subsequent cycle was run after 20%O_2/He reoxidation at 350 °C for 0.5 h

[b] T_r is the peak temperature of the main reduction peak

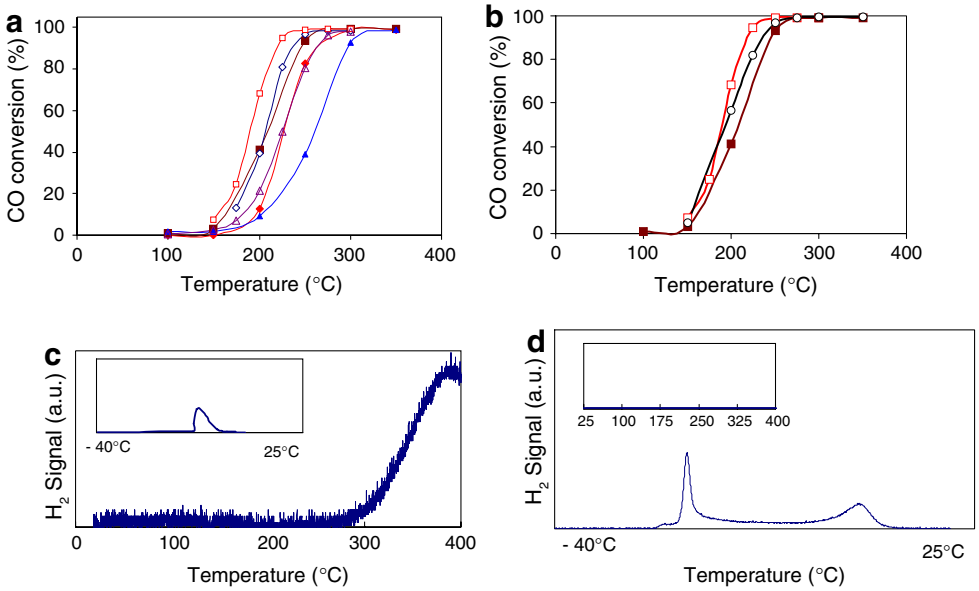

Fig. 6 (**a**) WGSR light-off over the Pt-ceria catalysts; steady-state conversion measurements. Gas mixture: 2%CO–10.7%H_2O–He; contact time: 0.09 g s/cc. Closed triangles—2.2%PtCeLaO$_x$ (IMP); Open triangles—in situ H_2 reduced 2.2%PtCeLaO$_x$ (IMP); Closed squares—5.3%PtCeO$_x$ (UGC); Open squares—in situ H_2 reduced 5.3%PtCeO$_x$ (UGC); Closed diamonds—1.1%PtCeO$_x$ (UGC), Open diamonds—in situ H_2 reduced 1.1%PtCeO$_x$ (UGC). In situ H_2 reduction: 20%H_2 at 5 °C/min from RT to 400 °C; Cooled to 300 °C in He for 30 min; WGSR tests from 300 °C to 150 °C in descending temperature mode. (**b**) WGS light-off over the 5.3%PtCeO$_x$ catalyst after various pretreatments; steady-state conversion measurements. Gas mixture: 2%CO–10.7%H_2O–He; contact time: 0.09 g s/cc. Closed squares—Fresh 5.3%PtCeO$_x$ (UGC); Open squares—in situ H_2 reduced 5.3%PtCeO$_x$ (UGC); Open Circles—in situ Oxidized 5.3%PtCeO$_x$ (UGC); In situ H_2 reduction: 20%H_2 at 5 °C/min from RT to 400 °C; Cooled to 300 °C in He for 30 min; WGSR tests from 300 °C to 150 °C in descending temperature mode. In situ Oxidation: 20%O_2 at 350 °C for 0.5 h; Cooled to 150 °C in He for 30 min; WGSR tests from 150 °C to 300 °C in ascending temperature mode. (**c**) H_2-TPR of used 5.3%PtCeO$_x$ (UGC). Used sample was recovered following in situ H_2 reduction/WGS reaction test at the conditions of **a**. The sample was purged in He at RT for 0.5 h before the H_2-TPR test. (**d**) H_2-TPR of used 1.1%PtCeO$_x$ (UGC). Used sample was recovered following in situ H_2 reduction/WGS experiment at the conditions of **a**. The sample was oxidized at 350 °C in 20%O_2 for 0.5 h, followed by RT He sweep for 0.5 h before the H_2-TPR test

material was pre-treated at 350 °C in oxygen followed by a helium sweep prior to starting the TPR test. In Fig. 6d, this sample only had the sub-RT reduction profile with a hydrogen consumption of 615 μmol/g_{cat}. We attribute this difference to carbonate formation. The He purge alone could not remove the carbonates from the 5.3%Pt sample. Upon exposure to high temperature (>250 °C) during the TPR test, the carbonate was reduced allowing for further ceria surface reduction and hydrogen consumption. By contrast, the used 1.1%PtCeO$_x$ had its carbonates removed by the 350 °C-oxygen, treatment, and its TPR profile (Fig. 6d) was similar to the second TPR cycle of this sample shown in Fig. 5b. While the carbonate presence lowers the catalyst activity, there is no long-term effect on the catalyst stability as the data of Fig. 3a demonstrate.

3.4 Stability in Shutdown-startup Operation

The stability of PtCeO$_x$ catalysts was further evaluated in shutdown/re-start cycles to simulate realistic fuel cell operation. In an earlier study, we found that the formation of cerium(III) hydroxycarbonate causes the deactivation of gold-ceria catalysts during shutdown—startup [8, 31]. However, we showed that addition of a small amount of oxygen in the WGSR gas mixture could inhibit the formation of cerium hydroxycarbonate, thus preventing the gold-ceria catalyst deactivation. By contrast, addition of 0.5% O_2 in a gas mixture of 10%CO–10%H_2O–60%H_2–7%CO_2–He did not stabilize the WGS activity of a Pt–CeLaO$_x$ sample [31]. It is possible that the oxygen potential in this particular gas mixture with very high H_2 content (60%) is not high enough to keep Pt–CeO$_x$ surface free of carbonate. In Fig. 7a, the oxygen potential was changed by varying the ratio of O_2 to H_2. For the first 120 min, the reaction was carried out in the reformate gas mixture of 11% CO–26% H_2O–26% H_2–7% CO_2–He. After steady state was reached at 300 °C, the sample was cooled to room temperature and held for 2 h before it was reheated to 300 °C; all in the same flowing gas mixture. Addition of 1%O_2 in this gas mixture was enough to stabilize the 2.2%PtCeLaO$_x$ (IMP) catalyst and to prevent its deactivation. The higher concentration of oxygen gave better activity recovery than 0.5%O_2, which confirms that

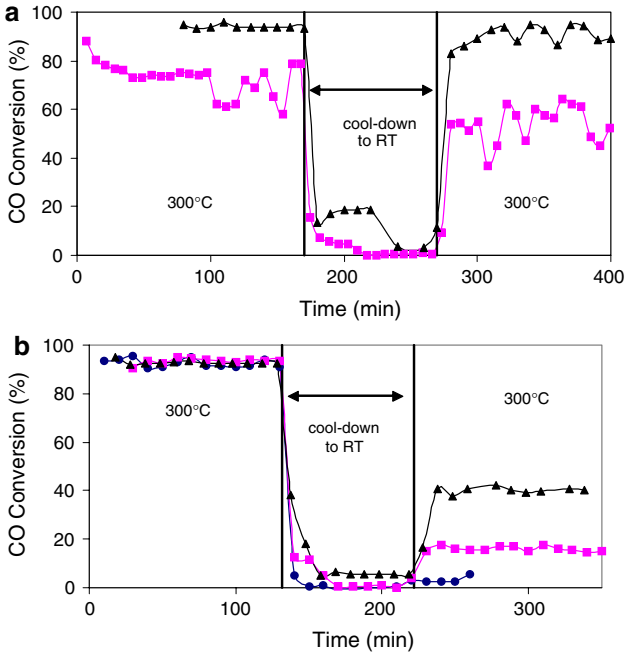

Fig. 7 WGSR shutdown/startup operation over (**a**) 2.2%PtCeLaO$_x$ (IMP) and (**b**) 5.3%PtCeO$_x$ (UGC) catalysts under various oxygen concentrations. Feed gas mixture: 11%CO–26%H_2–26%H_2O–7%CO_2–He; S.V. = 50,000 h^{-1}; catalyst was tested at 300 °C for 2 h, cooled to room temperature during shutdown with gas flowing for approximately 2 h, then reheated to 300 °C. (a) squares: 0.5% O_2 in feed gas; triangles: 1.0%O_2 in feed gas. (b) circles: no O_2 in feed gas; squares: 0.5% O_2 in feed gas; triangles: 1.0%O_2 in feed gas

the oxygen potential is the key factor that controls the deactivation of ceria-based catalysts.

Interestingly, the UGC-prepared 5.3%PtCeO$_x$ requires an even higher oxygen partial pressure to be fully stabilized. As shown in Fig. 7b, when the oxygen content was varied from 0 to 0.5% and 1%, respectively, the activity recovery of this material varied from less than 5–20% and 40%. Compared to Au-ceria, Pt-ceria catalysts require a higher oxygen potential reaction gas to stabilize their WGS activity. This may be attributed to the over-reduction of ceria caused by platinum [26]. On the other hand, using lanthanum as a cerium oxide dopant, appears to be beneficial, judging from the higher shutdown/re-start stability of the 2.2%PtCeLaO$_x$ sample (comparing Fig. 7a and b). More detailed work on how different dopants may prevent the cerium carbonate formation is warranted.

4 Conclusions

Platinum–cerium oxide catalysts can be prepared by various methods, including IMP, DP and UGC, in a form that is both active and stable in low-temperature WGSR. The UGC method is particularly well suited to prepare nanoscale ceria with a higher amount of oxidized Pt species strongly bound to ceria. The interaction produces finer ceria nanoparticles and a higher amount of reactive surface oxygen. Activity is higher if either hydrogen or oxygen gas is used to pre-treat the catalysts, indicating the importance of carbonate removal from the catalyst surface. The oxidation state of the surface Pt species is determined by the oxidation potential of the reaction gas mixture. Some, but not all the platinum is in metallic state after use. This can be reoxidized by heating to temperatures up to 350 °C.

Oxygen gas addition (~1 mol%) in the reformate gas mixture can be used to inhibit the deactivation of the PtCeO$_x$ catalysts during RT shutdown/re-start cycles. Oxygen prevents the formation of cerium(III) hydroxycarbonate at low temperatures. The amount required may be related to the number of redox sites of ceria, but more work is required to probe this. Non-etheless, active and stable catalysts based on nanoscale ceria doped with a small amount of platinum can be developed for practical fuel cell applications.

Acknowledgments This work was supported by the National Science Foundation, NIRT Grant # 0304515; and by the Department of Energy, Basic Energy Sciences, Hydrogen Fuel Initiative Grant # DE-FG02-05ER15730. The authors would like to thank Elisabeth Shaw at MIT Center for Materials Science and Engineering for her help with the XPS analysis and Yanping Zhai for some of the WGS reaction rate measurements.

References

1. Shelef M, George W, Graham W, McCabe RW (2002) In: Trovarelli A (ed) Catalysis by ceria and related materials, Catalytic Science Series, vol 2. Imperial College Press, p 343
2. Zhu T, Kundakovic Lj, Dreher A, Flytzani-Stephanopoulos M (1999) Catal Today 50:381
3. Liu W, Flytzani-Stephanopoulos M (1995) J Catal 153:304
4. Liu W, Flytzani-Stephanopoulos M (1995) J Catal 153:317
5. Murrell LL, Tauster SJ, Anderson DR (1991) In: Crucq A (ed) Catalysis and automotive pollution control II. Elsevier Science Publishers, p 275
6. Hardacre C, Ormerod RM, Lambert RM (1994) J Phys Chem 98:10901
7. Fu Q, Saltsburg H, Flytzani-Stephanopoulos M (2003) Science 301:935
8. Fu Q, Deng W, Saltsburg H, Flytzani-Stephanopoulos M (2005) Appl Catal B 56:57
9. Yao H-C, Yu Yao FY (1984) J Catal 86:254
10. Bunluesin T, Cordatos H, Gorte RJ (1995) J Catal 157:222
11. Bunluesin T, Gorte RJ, Graham GW (1998) Appl Catal B 15:107
12. Kundakovic Lj, Flytzani-Stephanopoulos M (1998) J Catal 179:203; Martínez-Arias A, Fernández-García M, Gálvez O, Coronado JM, Anderson JCA, J Cataluña, Conesa R, Soria JC, Munuera G (2000) J Catal 195:207
13. Li Y, Fu Q, Flytzani-Stephanopoulos M (2000) Appl Catal B 27:179
14. Avgouropoulos G, Ioannides T, Papadopoulou C, Batista J, Hocevar S, Matralis HK (2002) Catal Today 75:157
15. Fu Q, Weber A, Flytzani-Stephanopoulos M (2001) Catal Lett 77(1–3):87

16. Tabakova T, Boccuzzi F, Manzoli M, Andreeva D (2003) Appl Catal A 252(2):385
17. Tabakova T, Boccuzzi F , Manzoli M, Sobczak JW, Idakiev V, Andreeva D (2004) Appl Catal B 49:73
18. Fu Q, Kudriavtseva S, Saltsburg H, Flytzani-Stephanopoulos M (2003) Chem Eng J 93:41
19. Fu Q (2004) Ph.D. dissertation, Department of Chemical and Biological Engineering, Tufts University, Medford, MA
20. Yeung CMY, Yu KMK, QJ Fu D Thompsett, Petch MI, Tsang SC (2005) JACS 127(51):18010
21. Chiang YM, Lavik EB, Kosacki I, Tuller HL, Ying JY (1997) J Electroceramics 1:7
22. Kek-Merl D, Lappalainen J, Tuller HL (2006) J Electrochem Soc 153(3):J15
23. Carretin S, Concepcion P, Corma A, Lopez Nieto JM, Puntes VF (2004) Angew Chem Int Ed 43:2538
24. Guzman J, Carretin S, Corma A (2005) JACS 127:3287
25. Kim CH, Thompson LT (2005) J Catal 230:66
26. Zalc JM, Sokolovskii V, Loffler DG (2002) J Catal 206:169
27. Wang X, Gorte RJ, Wagner JP (2002) J Catal 212:225
28. Hillaire S, Wang X, Luo T, Gorte RJ, Wagner JP (2001) Appl Catal A 215:271
29. Liu X, Ruettinger W, Xu X, Farrauto R (2005) Appl Catal B 56:69
30. Ruettinger W, Liu X, Farrauto R (2002) US patent 141938
31. Deng W, Flytzani-Stephanopoulos M (2006) Angew Chem Int Ed 45:2285
32. Deng W, De Jesus J, Saltsburg H, Flytzani-Stephanopoulos M (2005) Appl Catal A 291:126
33. Deng W (in progress) Ph.D. thesis
34. http://www.webelements.com
35. Zhang F, Chan S-W, Spanier JE, Apak E, Jin Q, Robinson RD, Herman IP (2002) Appl Phys Lett 80(1):127
36. Manzoli M, Boccuzzi F, Chiorino A, Vindigni F, Deng W, Flytzani-Stephanopoulos M (2007) J Catal 245(2):308